NIH-PA Author Manuscript

NIH-PA Author Manuscript

NIH-PA Author Manuscript

NIH Public Access
Author Manuscript
J Cereb Blood Flow Metab. Author manuscript; available in PMC 2010 April 12.

Published in final edited form as:
J Cereb Blood Flow Metab. 2007 May ; 27(5): 909–918. doi:10.1038/sj.jcbfm.9600419.

Transport pathways for clearance of human Alzheimer's amyloid β-peptide and apolipoproteins E and J in the mouse central nervous system

Robert D. Bell[1,*], **Abhay Sagare**[1,*], **Alan E. Friedman**[2], **Gurrinder Bedi**[2], **David M. Holtzman**[3], **Rashid Deane**[1], and **Berislav V. Zlokovic**[1]

[1]Frank P. Smith Laboratory for Neuroscience and Neurosurgical Research, Department of Neurosurgery, University of Rochester Medical Center, Rochester, New York

[2]Department of Biochemistry and Biophysics, University of Rochester Medical Center, Rochester, New York

[3]Department of Neurology, Molecular Biology & Pharmacology, Washington University Medical School, St. Louis, Missouri.

Abstract

Amyloid β-peptide (Aβ) clearance from the central nervous system (CNS) maintains its low levels in brain. In Alzheimer's disease, Aβ accumulates in brain possibly due to its faulty CNS clearance and a deficient efflux across the blood-brain barrier (BBB). By using human specific ELISAs, we measured a rapid 30 min efflux at the BBB and transport via the interstitial fluid (ISF) bulk flow of human unlabeled Aβ and of Aβ transport proteins, apolipoprotein E (apoE) and apoJ, in mice. We show: (i) Aβ40 is cleared rapidly across the BBB via low density lipoprotein receptor related protein-1 at a rate of 0.21 pmol/min/g ISF or 6-fold faster than via the ISF flow; (ii) Aβ42 is removed across the BBB at a rate 1.9-fold slower than Aβ40; (iii) apoE, lipid-poor isoform 3, is cleared slowly via the ISF flow and across the BBB (0.03-0.04 pmol/min/g ISF), and after lipidation its transport at the BBB becomes barely detectable within 30 min; (iv) apoJ is eliminated rapidly across the BBB (0.16 pmol/min/g ISF) via low density lipoprotein receptor related protein-2. Clearance rates of unlabeled and corresponding ^{125}I-labeled Aβ and apolipoproteins were almost identical, but could not be measured at low physiological levels by mass spectrometry. Aβ40 binding to apoE3 reduced its efflux rate at the BBB by 5.7-fold, whereas Aβ42 binding to apoJ enhanced Aβ42 BBB clearance rate by 83%. Thus, Aβ, apoE and apoJ are cleared from brain by different transport pathways, and apoE and apoJ may critically modify Aβ clearance at the BBB.

Keywords

blood-brain barrier; clearance; amyloid β-peptide; apolipoprotein E; apolipoprotein J; mice

Introduction

Aβ accumulation in brain and its neuronal toxicity contribute to the pathogenesis and progression of Alzheimer's disease (AD) (Hardy and Selkoe, 2002; Zlokovic, 2005). Recent studies from our and other laboratories suggest a major role of Aβ clearance in determining

Address for Correspondence: Berislav V. Zlokovic, M.D., Ph.D. University of Rochester Medical Center 601 Elmwood Avenue, Box 645 Rochester, New York 14642 Phone:585.273.3132; Fax: 585.273.3133 berislav_zlokovic@urmc.rochester.edu.
*R. Bell and A. Sagare equally contributed to this work.

NIH-PA Author Manuscript

NIH-PA Author Manuscript

NIH-PA Author Manuscript

Aβ concentration in the CNS (Selkoe, 2001; Zlokovic, 2004; Tanzi et al., 2004; Zlokovic et al., 2005; Holtzman and Zlokovic, 2006). In particular, bi-directional transport of soluble free Aβ across the blood-brain barrier (BBB) via low density lipoprotein receptor related protein-1 (LRP1) (Shibata et al., 2000; Deane et al., 2004) and receptor for advanced glycation end products (Mackic et al., 1998a; Deane et al., 2003), binding of Aβ to apolipoprotein E (apoE) (Mackic et al., 1997) and apoJ (Zlokovic et al., 1996), Aβ metabolism (Selkoe, 2001; Iwata et al., 2000; Iwata et al., 2001) and degradation by astrocytes (Wyss-Coray et al., 2003; Koistinaho et al., 2004) may influence Aβ transport exchange at the BBB and/or its clearance from the CNS.

A microdialysis technique has been developed to measure transport exchange of an endogenous soluble pool of human Aβ in brain interstitial fluid (ISF) in different transgenic models of AD (Cirrito et al., 2003). On the other hand, the BBB bi-directional transport of exogenous soluble human Aβ (Zlokovic et al., 1993; Maness et al., 1994; Ghilardi et al., 1996; Ghersi-Egea et al., 1996; Poduslo et al., 1997; Mackic et al., 1998b; Deane et al., 2003; Banks et al., 2003; Deane et al., 2004; LaRue et al., 2004; Deane et al., 2005) and the BBB influx of its circulating binding transport proteins (Zlokovic et al., 1996; Mackic et al., 1997) have been frequently studied with ^{125}I-radiolabeled tracers. However, the clearance transport pathways of unlabeled exogenous Aβ and apolipoproteins from brain ISF have not been studied.

Here, we modified our well established clearance technique in mice (Shibata et al., 2000; Deane et al., 2004; Deane et al., 2005) to determine transport routes and clearance rates across the BBB and via the ISF bulk flow of unlabeled synthetic human Aβ40 and Aβ42 and of Aβ transport proteins, human recombinant apoE (isoform 3) and native human plasma-derived apoJ. To determine clearance of unlabeled test-molecules from the CNS we used human specific ELISAs. We have also explored the feasibility of matrix assisted laser desorption ionization time of flight (MALDI-TOF) mass spectrometry and liquid chromatography electrospray ionization mass spectrometry (LC-ESI MS/MS) to determine clearance of unlabeled Aβ and apolipoproteins from the CNS. Finally, we compared clearance rates of unlabeled and ^{125}I-labeled Aβ and apolipoproteins. Our data indicate Aβ, apoE and apoJ are cleared from brain by different transport routes, and binding of Aβ to apoE and apoJ may critically influence Aβ efflux at the BBB and its clearance from brain.

MATERIALS AND METHODS

Aβ and apolipoproteins

Aß40 and Aβ42 were synthesized and characterized as we described (Deane et al., 2004). Affinity purified crude extract of human plasma apoJ (Fig. 1a) was purified by High Pressure Liquid Chromatography (HPLC) (Fig. 1b), as described (de Silva et al., 1990; Zlokovic et al., 1996). The Tris/Tricine SDS-PAGE (10%-20%) shows a single apoJ band consisting of α and β chain (Fig. 1c) confirmed as apoJ by MALDI-TOF (not shown). Recombinant human apoE (isoform 3) was from baculovirus transfected Sf9 cells purchased from Invitrogen (Carlsbad, California, USA Cat. no. P2003). Lipidated apoE (isoform 3) was prepared from conditioned media of immortalized mouse astrocytes, as we described (Morikawa et al., 2005). Lipid-poor apoE complex with synthetic human Aβ40 was prepared as we described (Martel et al., 1997) and purified by the size exclusion Fast Protein Liquid Chromatography (FPLC) to remove excess Aβ. Aβ42-apoJ complex was prepared as we described (Zlokovic et al., 1996) and purified over an FPLC column prior to use. Within the 30 min of Aβ-apoE and Aβ-apoJ complex administration into brain ISF, Aβ in PBS soluble brain supernatant fraction co-immunoprecipitates with anti-apoE (3D12, Biodesign International, Sako, ME, USA Cat. no. H61529M) or anti-apoJ (A241, Quidel, San Diego, CA) antibody > 98% and 99%, respectively, indicating that the peptide remains stable in the form of complexes with apolipoproteins over the period required for clearance measurements.

NIH-PA Author Manuscript

NIH-PA Author Manuscript

NIH-PA Author Manuscript

Clearance technique

Mice were kept under standard housing conditions and feeding schedules until experimental procedures were performed. All studies were performed according to the National Institutes of Health guidelines using an approved institutional protocol. Briefly, a stainless steel guide cannula was implanted stereotaxically into the right caudateputamen of anesthetized mice (100 mg/kg ketamine and 10 mg/kg xylazine i.p.) with the cannula tip coordinates 0.9 mm anterior and 1.9 mm lateral to the bregma and 2.9 mm below the surface of the brain. Animals were recovered after surgery before clearance studies. The experiments were performed before substantial chronic process occurred, as assessed by histological analysis of tissue, i.e., negative staining for astrocytes (glial fibrillar acidic protein) and activated microglia (anti-phosphotyrosine), but allowing time for the BBB repair for large molecules, as reported previously (Cirrito et al., 2003; Deane et al., 2004; Deane et al., 2005).

The test-molecules, unlabeled synthetic human Aβ40 and Aβ42, human apoE (isoform 3) non-lipidated and lipidated, and human native apoJ were administered into brain ISF simultaneously with ^{14}C-inulin (reference molecule) over 5 min using our clearance technique (Shibata et al., 2000). The test-molecules were administered in 0.5 μL mock ISF at equimolar concentration of 40 fmol/μL corresponding to 0.173 and 0.181 ng/μL of Aβ40 and Aβ42, respectively, 1.40 ng/μL of apoE, non-lipidated or lipidated, and 3.20 ng/μl of apoJ. When the effects of anti-LRP1 (N20, polyclonal goat anti-human antibody that cross-reacts with mouse LRP1; Santa Cruz Biotech. Inc. Santa Cruz, CA), anti-LRP2 (low density lipoprotein receptor related protein-2; Rb 6286, from Dr. S. Argraves) and control non-immune IgG (NI IgG; murine serum IgG, Sigma, St. Louis, MO) on Aβ or apoJ clearance were studied, these were infused at concentration of 60 μg/mL 10 min prior to and then simultaneously with the test-molecules. Receptor associated protein (RAP) (Oxford Biomed Research, Oxford, MI) which blocks both LRP1 (Shibata et al., 2000; Deane et al., 2004) and LRP2 (Zlokovic et al., 1996) was infused at 5 μM 10 min prior to and then simultaneously with the test-molecules. Clearance of Aβ, apoE and apoJ was determined focally in brain by using human specific ELISAs (see below). At predetermined times, which in most experiments was within 30 min of intracerebral administration, brain and blood were sampled and prepared for Aβ, apoE and apoJ ELISAs.

In studies with ^{125}I-labeled test-molecules, the amount of injected tracers was determined using a micrometer to measure the linear displacement of the syringe plunger in the precalibrated micro-syringe. Tracer fluid (0.5 μL) containing [^{125}I]-labeled test-molecules (e.g., Aβ, apolipoproteins) and ^{14}C-inulin (reference molecule) was injected over 5 minutes. To directly compare the clearance rates of ^{125}I-labeled Aβ and apolipoproteins with the corresponding unlabeled Aβ and apolipoproteins, we administered exactly the same amounts of ^{125}I-labeled Aβ40 (0.173 ng/μL), Aβ42 (0.181 ng/μL), apoE (1.40 ng/μL) non-lipidated and lipidated isoform 3, and apoJ (3.20 ng/μL), as in the experiments with unlabeled Aβ and apolipoproteins. Brain and blood were sampled and prepared for radioactivity analysis as described (Shibata et al., 2000; Deane et al., 2005). Clearance of Aβ, apoE and apoJ was determined by the radioactivity analysis (see below).

Detection of clearance by human specific ELISAs

Briefly, about 15 mg of brain tissue adjacent to the site of microinjection was homogenized with an extraction buffer containing 50 mM NaCl, 0.2% diethylamine (DEA) and complete protease inhibitor cocktail (Roche Indianapolis, IN). DEA was used since it improves Aβ recovery from tissue homogenates, reduces background signal and requires low dilution prior to ELISA determination (Schmidt et al., 2005). This allows for quantification of typically low levels of soluble Aβ found in tissues without plaques (Best et al., 2005; Deane et al., 2005). Samples were centrifuged for 1 hr at 100,000 g, and supernatant (pH 8.0) diluted 1:1 before adding to ELISA plates. Aβ 1-40 and 1-42 colorimetric kits (Invitrogen, KHB3441 and

NIH-PA Author Manuscript

NIH-PA Author Manuscript

NIH-PA Author Manuscript

KHB3544) were used to determine Aβ40 and Aβ42 levels in brain extract and plasma, respectively. These kits detect whole intact Aβ 1-40 and 1-42 molecules and do not recognize Aβ fragments. For apoE and apoJ, polysterene microtiter plates were coated with 10 μg/mL monoclonal anti-apoE antibody (3D12) or polyclonal anti-apoJ antibody (Chemicon, Temecula, CA), respectively overnight at 4 °C. After blocking with 3% BSA for 1 hr at room temperature, standards and samples were added and incubated for 2 hr. Bound apoE and apoJ were detected by affinity-purified biotinylated goat anti-apoE (Biodesign Cat. No. K74180B) and monoclonal anti-apoJ (Quidel, Cat. No. A241) antibodies, respectively, followed by streptavidin-HRP conjugate (Invitrogen, Cat. No. SNN2004) or anti mouse-HRP conjugate (Sigma, Cat. No. A4789). The reaction was developed for 30 min using tetramethyl benzidine substrate and stopped with 1N HCl and quantified at 450 nm. The recovery of test-molecules at time zero (immediately after administration) was > 99% which compares well with the recovery of ^{14}C-inulin (> 99%) determined by the liquid scintillation spectrometry. To determine the levels of simultaneously injected ^{14}C-inulin, 15 μL of the brain extract was solubilized in 0.5 mL of tissue solubilizer (PerkinElmer, Boston, MA) overnight before the addition of 5 mL of scintillation fluid (Packard Utima Gold, PerkinElmer), and analyzed in a liquid scintillation counter (Packard Tri-Carb 2100TR Liquid Scintillation Counter, PerkinElmer). The levels of Aβ40 and apoE in brain after administration of preformed Aβ40-apoE complex were determined as described above using 25 μL of the brain extract for each ELISA.

Detection of clearance with iodinated ligands

Aβ40 and 42 were iodinated using a mild lactoperoxidase method (LeRue et al., 2004). Radiolabled peptides were HPLC purified to eliminate free iodide, di-iodinated Aβ, oxidized Aβ or unlabeled Aβ, as we reported (Deane et al., 2003; LaRue et al., 2004). For clearance studies, we used only reduced monoidinated Aβ peak (specific activity ~ 60 μCi/μg), as confirmed by MALDI-TOF mass spectrometry analysis, as reported (LaRue et al., 2004). ApoJ and apoE were labeled by Iodo-Gen (Pierce, Rockford, IL, Cat. No. 28600) to specific activity of 9-12 μCi/μg. Free iodide was removed from radiolabeled apoE and apoJ preparations by gel-filtration. All ^{125}I-labeled molecules were used within 24 hr of labeling to avoid radiolysis, as we described (LaRue et al., 2004). The trichoracetic acid (TCA)-precipitable ^{125}I-radioactivity and the non-TCA precipitable ^{125}I-radioactivity (e.g., degraded Aβ) were determined, as we reported (Shibata et al., 2000; Deane et al., 2003; Deane et al., 2004). Our earlier studies with ^{125}I-labeled Aβ have demonstrated that both radiolabeled Aβ40 and Aβ42 remain mainly intact in brain ISF (> 95%) within 30-90 min of *in vivo* clearance studies (Shibata et al., 2000), as well as during rapid clearance studies *in vitro* on brain capillaries (Deane et al., 2004), as shown by the TCA analysis and confirmed by the HPLC and SDS-PAGE analyses. In the present study, the TCA, HPLC and SDS-PAGE/immunoprecipitation analysis confirmed pervious findings indicating that molecular forms of transport of ^{125}I-labeled Aβ and apolipoproteins within 30 min of clearance studies remained mainly in their original form of intact molecules (> 98%), as injected in the CNS.

MALDI-TOF and LC ECI MS/MS

To determine the limit of quantification (LOQ) for human Aβ by MALDI-TOF mass spectrometry, we spiked mouse CSF with various amounts of human synthetic Aβ40 (0.1 – 30 ng per spot) and a constant amount of metabolically labeled ^{15}N-Aβ40 (internal standard; 30 ng per spot; R-peptide, Atlanta, GA), as reported (Gelfanova et al., 2006). Samples were mixed with an equal volume of α-cyano-4-hydroxycinnamic acid in 50 % acetonitrile and spotted onto the MALDI target using a MALDI-TOF MS (Voyager-DE STR BioSpectrometry Applied Bioscience, Foster City, CA). Spectra were obtained from 15 separate areas of the spot with 200 laser shots per acquisition. All acquisitions were averaged for each spot.

NIH-PA Author Manuscript

NIH-PA Author Manuscript

NIH-PA Author Manuscript

For LC-ESI MS/MS analysis, ^{15}N-Aβ40 was digested into tryptic peptides and applied to a microcapillary liquid chromatography system (Surveyor MS Pump Plus HPLC system Thermo Corporation, San Jose, CA) coupled to the linear ion-trap mass spectrometer (Thermo Corporation, San Jose, CA). An in-line analytical capillary column (75 μm id 10 cm) was packed using C_{18} reversed-phase resin (5 μm, 200 Å Magic C_{18}AG, Michrom BioResource, Auburn, CA) and Picofrit capillary tubing (75 μm ID 10 cm, New Objective, Cambridge, MA). Each sample was first concentrated and de-salted by loading in solvent A (0.1% acetic acid in solution of 5% acetonitrile and 95% water) for 20 minutes. Peptides were eluted using a linear gradient of 5-70% solvent B (to a final working concentration 0.1% acetic acid in solution of 95% acetonitrile and 5% water over 70 min, followed by isocratic elution at 95% solvent B for 10 min, to wash the column, with a flow rate of 0.200 μL/min across the column. Peptides eluting from the capillary column were automatically selected for collision induced dissociation (CID) by the mass spectrometer using a data-dependent protocol that alternated between one MS scan and seven MS/MS scans for the seven most abundant precursor ions detected in the MS survey scan. Precursor *m/z* values, selected for CID using a collision energy setting of 35%, were dynamically excluded for 30 sec after selection. The mass range for precursor ion detection was set from 400 to 2000 Dalton. The electrospray voltage was set to 2.1 kV. The operation of the mass spectrometer was controlled by Xcalibur LC/MS/MS software (Thermo Corporation, San Jose, CA). The MS/MS spectra were sequence database searched using a database that had been indexed using ^{15}N modifications via SEQUEST7 and Bioworks Browser (both from Thermo Corporation, San Jose, CA). Default threshold cutoffs were made using the following parameters: normalized cross correlation score for +1, +2, and +3 charge peptides of 1.9, 2.7 and 3.5 respectively, and a DeltaCN value of 0.1. The MS/MS spectra were searched against a downloaded non-redundant human proteome sequence database from European Bioinformatics Institute (http://www.ebi.ac.uk/IPI/IPIhuman.html) to determine possible sequence correlations of known proteins for identification.

Mathematical modeling

Transport clearance rates of unlabeled test-molecules, i.e., Aβ, apoE and apoJ, across the BBB and by the ISF bulk flow were determined from the respective ELISA measurements by using transport analysis similar to that as reported for radiolabeled test-molecules (Shibata et al., 2000; Deane et al., 2004). The concentrations of unlabeled test-molecules in brain at time zero and at pre-determined clearance times t were expressed in pmol/g ISF, assuming 1 g of brain contains 0.1 g of ISF (Zlokovic, 2005; Deane et al., 2005). Brain recovery of studied test-molecules and of simultaneously infused ^{14}C-inulin (reference molecule) was calculated as

$$100 \times N_t/N_0 \qquad \text{(eq. 1)}$$

, where N_t is the concentration of the test molecule or the amount of inulin at the end of experiment at time t, and N_0 is the concentration of a test-molecule or the amount of inulin injected in brain ISF at time zero (Shibata et al., 2000). The fractional clearance rate constant of inulin (k, min^{-1}) provides measure of the ISF bulk flow (Shibata et al., 2000), and is calculated as

$$N_t\,(\text{inulin})\,/N_0\,(\text{inulin}) = \exp\,(-k\,\text{inulin}^{*}t) \qquad \text{(eq. 2)}$$

. In a case of Aβ multiple-time efflux series with departure of the later time points (> 30 min) from the linear efflux phase, the concentration of unlabeled Aβ in brain ISF (pmol/g ISF) at time t ($Aβ_t$) is related to the concentration of Aβ at time zero ($Aβ_0$) and the rates of Aβ total efflux from brain (k1) and its retention in brain (k2) by the bi-exponential equation,

$$A\beta_t = A\beta_0\left[a1 + a2e^{-(k(1))t}\right] \quad \text{(eq. 3)}$$

, where a1 = k2 / (k1+ k2) and a2 = k1 / (k1+ k2), and k1 and k2 are expressed in pmol Aβ/min/g ISF, as reported for radiolabeled Aβ (Shibata et al., 2000). In a case of single-time point rapid efflux series within the 30 min of the linear efflux of test-molecules from brain, the concentrations of unlabeled Aβ, apoE and apoJ, in brain ISF (pmol/g ISF) at 30 min (test-molecule$_{t30}$) are related to the concentrations of the respective test-molecules at time zero (test-molecule$_{t0}$) and the total rate of efflux (k3, pmol test-molecule/min/g ISF) by the mono-exponential equation,

$$\text{test}-\text{molecule}_{t30} = \exp\left(-k3\left[\text{test}-\text{molecule}_{t0}\right]^{*} t_{30}\right) \quad \text{(eq. 4)}$$

, as reported for radiolabeled Aβ (Deane et al., 2004). The clearance rates of Aβ, apoE and apoJ across the BBB (pmol/min/g ISF) were calculated from the single-time efflux series within 30 min from the total efflux rates of test-molecules (k3, pmol/min/g ISF; eq. 4) and the fraction of test-molecules cleared via the ISF bulk flow determined by the clearance rate of inulin (reference molecule) as:

$$k4 = k3(\text{test}-\text{molecule})_{t30} - k\,(\text{reference}) \times (\text{test}-\text{molecule}_{t0}) \quad \text{(eq. 5)}$$

, where test-molecule$_{t0}$ is the initial concentration of the test-molecule injected into brain ISF at time zero, t_0. The same equations were used to calculate clearance rates of radiolabeled test-tracers taking into account their respective concentrations, as we described (Shibata et al., 2000; Deane et al., 2004). In case of ^{125}I-labeled Aβ, apoE and apoJ, only ^{125}I TCA-precipitable radioactivity was used to calculate the concentrations of intact tracers.

Statistical analysis

Data are analyzed by multifactorial analysis of variance and Student's t test. The differences were considered to be significant at $p < 0.05$. All values were mean ± SEM.

RESULTS

Detection of human Aβ, apoE and apoJ clearance by human specific ELISAs

Fig. 2a shows disappearance curve of human synthetic unlabeled Aβ40 from brain after its administration into brain ISF simultaneously with ^{14}C-inulin over the studied period of time of 240 min. There was time-dependent and rapid disappearance of Aβ40 from its initial levels at time zero of about 13 pmol/g ISF to almost undetectable levels at 90 min, 120 min and 240 min. In contrast to Aβ, ^{14}C-inluin was cleared slowly from brain via the ISF bulk flow (Shibata et al., 2000;Deane et al., 2004), as indicated by its high brain retention of 74% and 52% of the injected dose at 90 min and 240 min, respectively. The levels of human Aβ40 and Aβ42 at the beginning of the clearance study at time zero, $A\beta_0$, were on average 12.8 and 13.2 pmol/g ISF, which was within the range of endogenous Aβ levels in the mouse brain, as reported (Deane et al., 2005) (Fig. 2b) Both, Aβ40 and Aβ42 levels decreased significantly within 30 min to 5.16 and 8.64 pmol/g ISF, respectively, indicating clearance from brain of both peptides, and significantly faster elimination of Aβ40. The drop in inulin within 30 min was ~ 10% reflecting its passive transport via the ISF flow (Shibata et al., 2000;Deane et al., 2004). Fig. 2c shows efflux of unlabeled Aβ at 30 min is significantly inhibited (> 70%) with centrally administered LRP1-specific antibody and RAP, but not with NI IgG or anti-LRP2 (not shown). Moreover,

NIH-PA Author Manuscript NIH-PA Author Manuscript NIH-PA Author Manuscript

intact human Aβ40 and Aβ42 were both present in mouse plasma within 30 min of CNS administration, but were undetectable in plasma in the presence of centrally administered LRP-1-specific antibody, as determined by the respective ELISAs (Fig. 2d). This data confirm transcytosis of intact Aβ peptides across the BBB and inidcate that Aβ efflux at the BBB is LRP1-dependent, as suggested by earlier work with radiolabeled Aβ (Shibata et al., 2000;Deane et al., 2004). It is of note, plasma levels of inulin were not significantly different form zero (not shown) consistent with its slow clearance via the ISF flow.

Fig. 3a shows the levels of non-lipidated apoE (isoform 3) were slightly reduced from 13.1 pmol/g ISF at time zero to 10.9 pmol/g ISF at 30 min. There was almost no difference in slope between inulin and lipidated apoE (isoform 3) within 30 min of their simultaneous administration into brain ISF. In contrast, apoJ was cleared rapidly across the BBB as indicated by a steep drop of its levels from 13.3 pmol/g ISF at zero time to 7.3 pmol/g ISF at 30 min (Fig. 3b). Fig. 3c shows that Aβ40 clearance from its pre-formed complex with lipid-poor apoE is reduced substantially at 30 min compared to clearance of free Aβ injected into brain ISF at equimolar concentration in the absence of apoE. In contrast to Aβ, the levels of apoE at 30 min of the CNS administration were comparable regardless of whether apoE (isoform 3) was injected alone or in the form of a complex with Aβ.

The rates of Aβ, apoE and apoJ efflux via BBB transport and the ISF flow were calculated from 30 min series by using eqs. 2, 4 and 5 and a transport kinetic model similar to that as we reported for radiolabeled Aβ (Shibata et al., 2000). Table 1 shows that transport via BBB represents a major efflux route for human Aβ40 from the CNS. The rate of BBB efflux of 0.21 pmol/min/g ISF was > 6-fold greater than the rate of its transport via the ISF flow consistent with the results obtained with ^{125}I-labeled Aβ40 (Shibata et al., 2000). The rate of Aβ clearance across the BBB calculated from the multiple-time efflux series (Fig. 2a) with eqs. 2, 3 and 4 was 0.22 pmol/min/g ISF, which was almost identical as the rate of Aβ BBB efflux obtained from a single time-point series (Table 1). We also showed that the rate of Aβ42 BBB efflux was 1.9-fold lower than for Aβ40, although its elimination via the ISF flow was comparable to that of Aβ40. Non-lipidated apoE (isoform 3) at its physiological CSF levels was transported via the ISF flow and across the BBB at comparable low rates, i.e., from 0.03 to 0.04 pmol/min/g ISF, respectively. There was no detectable rapid BBB efflux of lipidated apoE3 within 30 min, which does not rule out the possibility that lipidated apoE may be cleared from brain over longer periods of time > 30 min. At its physiological CSF levels of 40 fmol/μL[35], apoJ was cleared rapidly from brain ISF within 30 min mainly via BBB transport at a rate of 0.16 pmol/min/g ISF. Aβ40-apoE complex was cleared at the BBB at a rate 5.7-fold lower than free Aβ40.

Detection of human Aβ, apoE and apoJ clearance with radiolabeled tracers

Since earlier work on CNS transport of exogenous Aβ employed radiolabled Aβ, we next studied weather CNS clearance of ^{125}I-labeled Aβ40 and Aβ42, as well as of ^{125}I-labeled apoE and apoJ corresponds to clearance of the respective unlabeled test-molecules, as measured above. To directly compare the clearance rates of ^{125}I-labeled and unlabeled Aβ and apolipoproteins, we administered exactly the same amounts (ng/μL) of ^{125}I-labeled Aβ40, Aβ42, apoE and apoJ as in the experiments with unlabeled Aβ and apolipoproteins, as explained in Methods. Fig. 4a shows that within 30 min of the CNS administration brain recovery of the corresponding unlabeled and ^{125}I-labeled Aβ, apoE and apoJ molecules were almost identical. Table 2 shows that the clearance rates via BBB transport and ISF flow of ^{125}I-labeled Aβ40, Aβ42, apoE non-lipidated and lipidated isoform 3 and of apoJ over the 30 min period were not significantly different from the rates of their respective unlabeled molecules (see Table 1). This data suggests that iodination does not alter Aβ, apoE and apoJ clearance from the CNS. Fig. 4b shows that apoJ clearance from brain was inhibited by RAP and anti-LRP2, but not by anti-

NIH-PA Author Manuscript NIH-PA Author Manuscript NIH-PA Author Manuscript

LRP1, as indicated by significantly higher N_t/N_0 brain retention values for apoJ in the presence of RAP and anti-LRP2. Appearance of TCA-precipitable ^{125}I-radioactivity in plasma after administration of ^{125}I-apoJ into brain ISF suggested apoJ transport from brain ISF to blood, which has been confirmed with native unlabeled apoJ by a human specific apoJ ELISA (not shown). Since apoJ is cleared faster from brain ISF than Aβ42, we tested whether binding of Aβ42 to apoJ may increase Aβ42 clearance from the CNS. ^{125}I-Aβ42-apoJ complex was prepared as we described (Zlokovic et al., 1996). Fig. 4c shows that Aβ42 bound to apoJ was cleared faster than Aβ42 alone, and clearance of Aβ-apoJ complex was blocked by anti-LRP2-specific antibody. The rate of Aβ42-apoJ clearance across the BBB was increased by 83% compared to Aβ42 alone.

MALDI-TOF and LC ECI MS/MS analysis

By using the MALDI-TOF MS analysis, we obtained a LOQ of 8 ng/μL for exogenous human Aβ40 in mouse CSF or artificial ISF. Since physiological levels of exogenous Aβ in focal brain clearance studies are typically achieved with microinjections of 0.5 μL mock ISF containing 0.173 ng/μL or less of Aβ40 (Shibata et al., 2000; Deane et al., 2005), to achieve the LOQ it would require concentration of CSF and brain extracts from 920 and 231 mice, respectively. Using a more sensitive serial MALDI-TOF-TOF (Gelfanova et al., 2006), it would still require concentration of CSF from 12 mice and brain extracts from 3 mice to achieve the LOQ.

By using the LC-ESI MS/MS analysis, the LOQ for ^{15}NAβ40 was 0.1732 ng/μL in mouse CSF or artificial ISF. Therefore, in a typical brain clearance study with physiological focal levels of exogenous Aβ40, concentration of CSF from 20 mice and brain extracts from 5 mice would be required to achieve this LOQ. Regarding apoE, the LOQ was 1.4 ng/μL. Thus, in a typical clearance study with exogenous apoE at low physiological levels, the CSF from 20 mice and brain extracts from 3 mice would need to be concentrated to achieve this LOQ.

DISCUSSION

Our data suggest that one can measure accurately the clearance rates of unlabeled human Aβ and apolipoproteins across the BBB and via the ISF bulk flow in mice by using human specific ELISAs. MALDI-TOF mass spectrometry and LC ESI MS/MS were less sensitive than the ELISA measurements in determining the CNS clearance rates in mice of unlabeled Aβ and apolipoproteins at low physiological levels as found normally in the CSF and brain in mice and humans (DeMattos et al., 2003). The present study shows for the first time that iodination does not alter the CNS clearance measurements of Aβ 1-40 and 1-42, as long as transport of ^{125}I-labeled Aβ is measured in its monoiodinated reduced form, as reported (Deane et al., 2003; LaRue et al., 2004; Deane et al., 2004; Deane et al., 2005). Moreover, we show for the first time that apoE and apoJ are cleared from brain by different transport routes and at substantially different rates, that the clearance of lipidated apoE is much slower than non-lipidated apoE, and that binding of Aβ to these apolipoproteins may critically alter its clearance from the CNS.

The present study shows unlabeled Aβ40, at the levels corresponding to those of mouse endogenous brain Aβ(Deane et al., 2005), is removed rapidly from brain ISF via transport across the BBB at a rate of 0.21 pmol/min/g ISF. Transport of unlabeled Aβ40 at the BBB was mediated via LRP1, as found with ^{125}I-labeled Aβ40 (Shibata et al., 2000; Deane et al., 2004). Since the levels of soluble, rapidly exchangeable Aβ pool in brain ISF in AD mice are around 300 pmol/L ISF, as shown by microdialysis technique (DeMattos et al., 2003), given the Aβ BBB efflux rate as determined in the present study, it would take about 40 seconds for LRP1 to clear this Aβ pool from brain ISF, assuming Aβ central production and re-entry of circulating Aβ into the brain (Deane et al., 2003) stop. In AD models and AD the levels of total Aβ in brain including insoluble Aβ are in low micromolar range, as for example around 6

NIH-PA Author Manuscript
NIH-PA Author Manuscript
NIH-PA Author Manuscript

NIH-PA Author Manuscript

NIH-PA Author Manuscript

NIH-PA Author Manuscript

μmol/kg brain (Cirrito et al., 2003; DeMattos et al., 2003). Making assumptions as above, it would take under pathological conditions about 30 to 45 minutes for LRP1 at the BBB to eliminate all soluble free Aβ from brain ISF, and about 14 days to remove total Aβ from brain in AD, providing that all Aβ could be resolublized into its free form. Although these numbers suggest high BBB efflux capacity for free Aβ, the present study indicates that the major pathogenic species of Aβ, Aβ42 (Selkoe, 2001), is cleared at the BBB at a rate 1.9-fold slower than Aβ40. Earlier work suggested LRP1 expression at the BBB may be substantially reduced in AD and in AD models (Deane et al., 2004). Thus, both of these factors may further modify elimination times of free Aβ under pathological conditions.

We show lipid poor apoE (isoform 3) is cleared slowly from brain compared to Aβ40 or Aβ42 mainly because of its low transport at the BBB, i.e., 0.04 pmol/min/g ISF. Since a large part of the effect of apoE isoforms on AD and cerebral amyloid angiopathy risk is mediated by the interaction of apoE with Aβ (Holtzman and Zlokovic, 2006), and neither mouse apoE nor human apoE have an impact on synthesis of brain Aβ in AD models (Bales et al., 1997; Holtzman and Zlokovic, 2006), we hypothesized apoE must affect clearance of Aβ within or from brain. Our data show that binding of Aβ40 to apoE (isoform 3) reduces by 5.7-fold its efflux rate at the BBB. The present study has been focused on apoE3 and used relatively short clearance times within the periods of 30 min. There may be isoform-specific differences in apoE clearance from brain and in apoE-mediated retention of Aβ in brain that could possibly be revealed over the longer times allowed for the clearance measurements (> 30 min) than in the present study. It is well recognized that the ε4 allele has a gene-dose effect on the risk and age of onset of AD and the amount of deposited Aß40 and vascular Aβ load, as reviewed by Holtzman and Zlokovic (2006). The isoform-specific effect of apoE on clearance of lipid-poor and lipidated apoE, the effects of longer efflux times on apoE clearance and the receptors involved in mediating slow removal of apoE and apoE-Aβ complexes across the BBB, remain to be determined by future studies. It is interesting to note, it has been recently suggested that low density lipoprotein receptor (LDLR) may be involved in regulating the CNS levels of human and mouse endogenous apoE (Fryer et al., 2005) and amyloid pathology in AD mice (Cao et al., 2006).

Finally, we demonstrate that native apoJ is eliminated rapidly from brain ISF across the BBB at a rate lower than that of Aβ40, but significantly higher than the rate of Aβ42. ApoJ is the major carrier protein for Aß in biological fluids (Calero et al., 2000), and its receptor LRP2 is expressed at the BBB (Zlokovic et al., 1996; Chun et al., 1999). We hypothesized LRP2 may be involved in efflux of apoJ out of the CNS, and Aβ binding to apoJ may enhance clearance of highly pathogenic Aβ42. Our data show that both RAP and LRP2-specific antibody block apoJ clearance, indicating LRP2 is required for apoJ efflux at the BBB. We next show that binding of Aβ42 to apoJ accelerates Aβ42 clearance rate at the BBB by 83%, which again requires LRP2. It has been reported that LRP2 at the BBB is saturated from the blood side by physiological levels of apoJ in plasma which precludes brain influx of circulating Aβ bound to apoJ across the BBB (Zlokovic et al., 1996). In contrast, efflux of Aβ42-apoJ complex from brain ISF to blood is substantial at physiological apoJ CSF levels as shown in the present study suggesting the net-transport of Aβ via apoJ at the BBB favors its efflux from brain. Consistent with the present study are findings demonstrating that lack of apoJ in AD mice may increase levels of soluble Aβ in brain (DeMattos et al., 2004). Since apoJ increases Aβ neurotoxicity in AD mice (De Mattos et al., 2002), clearance of Aβ-apoJ complexes from brain could be neuroprotective.

In conclusion, the present study highlights the importance of Aβ clearance mechanisms in the CNS suggesting that efflux of Aβ form brain is controlled by different transport pathways at the BBB. The lipoprotein receptors seem to play a major role in determining the rate of Aβ efflux at the BBB, either in its free form via LRP1 and/or in its bound form as a complex with

apoJ via LRP2. Whether other lipoprotein receptors such as LDLR participate in slow clearance of Aβ-apoE complexes at the BBB remains to be explored. Future studies should characterize in greater detail possible role of apoE/LDLR transport interactions at the BBB and of apoJ/LRP2 interactions in regulating the levels of soluble, as well as of deposited Aβ in brain.

Acknowledgments

This research was supported by United States Public Health Service grants NS34467, R37AG13956 (DMH) and R37AG023084 (B.V.Z.)

References

Bales KR, Verina T, Dodel RC, Du Y, Altstiel L, Bender M, Hyslop P, Johnstone EM, Little SP, Cummins DJ, Piccardo P, Ghetti B, Paul SM. Lack of apolipoprotein E dramatically reduces amyloid β-peptide deposition. Nat Genet 1997;17:263–264. [PubMed: 9354781]

Banks WA, Robinson SM, Verma S, Morley JE. Efflux of human and mouse amyloid β–proteins1-40 and 1-42 from brain: impairment in a mouse model of Alzheimer's disease. Neurosci 2003;121:487–492.

Best JD, Jay MT, Otu F, Ma J, Nadin A, Ellis S, Lewis HD, Pattison C, Reilly M, Harrison T, Shearman MS, Williamson TL, Atack JR. Quantitative measurement of changes in amyloid-β(40) in the rat brain and cerebrospinal fluid following treatment with the α-secretase inhibitor LY-411575 [N^2-[(2S)-2-(3,5-difluorophenyl)-2-hydroxyethanoyl]-N^1-[(7*S*)-5-methyl-6-oxo-6,7-dihydroxyethanoyl]-N^1-[(7*S*)-5-methyl-6-oxo-6,7-dihydro-5*H*-dibenzo[b,d]azepin-7-yl]-L-alaninamide]. J Pharmacol Exp Ther 2005;313:902–908. [PubMed: 15743924]

Calero M, Rostegno A, Matsubara E, Zlokovic BV, Ghiso J. Apolipoprotein J (clusterin) and Alzheimer's disease. Micro Res Tech 2000;50:305–315.

Cao D, Fukuchi K, Wan H, Kim H, Li L. Lack of LDL receptor aggravates learning deficits and amyloid deposits in Alzheimer transgenic mice. Neurobiol Aging. 2006 (in press) doi:10.1016/j.neurobiolaging.2005.09.011.

Chun JT, Wang L, Pasinetti GM, Finch CE, Zlokovic. BV Glycoprotein 330/megalin (LRP-2) has low prevalence as mRNA and protein in brain microvessels and choroid plexus. Exp Neurol 1999;157:194–201. [PubMed: 10222122]

Cirrito JR, May PC, O'Dell MA, Taylor JW, Parsadanian M, Cramer JW, Audia JE, Nissen JS, Bales KR, Paul SM, DeMattos RB, Holtzman DM. *In vivo* assessment of brain interstitial fluid with microdialysis reveals plaque-associated changes in amyloid-β metabolism and half-life. J Neurosci 2003;23:8844–8853. [PubMed: 14523085]

de Silva HV, Stuart WD, Duvic CR, Wetterau JR, Ray MJ, Ferguson DG, Albers HW, Smith WR, Harmony JA. A 70-kDa apolipoprotein designated ApoJ is a marker for subclasses of human plasma high density lipoproteins. J Biol Chem 1990;265:13240–13247. [PubMed: 2376594]

Deane R, Du Yan S, Submamaryan RK, LaRue B, Javanovic S, Hogg E, Welch D, Manness L, Lin C, Yu J, Zhu H, Ghiso J, Frangione B, Stern A, Schmidt AM, Armstrong DL, Arnold B, Liliensiek B, Nawroth P, Hofman F, Kindy M, Stern D, Zlokovic BV. RAGE mediates amyloid-β peptide transport across the blood-brain barrier and accumulation in brain. Nat Med 2003;9:907–913. [PubMed: 12808450]

Deane R, Sagare A, Hamm K, Parisi M, LaRue B, Guo H, Wu Z, Holtzman DM, Zlokovic BV. IgG-assisted age-dependent clearance of Alzheimer's Aβ by the blood-brain barrier neonatal Fc receptor. J Neurosci 2005;25:11495–11503. [PubMed: 16354907]

Deane R, Wu Z, Sagare A, Davis J, Du Yan S, Hamm K, Xu F, Parisi M, LaRue B, Hu HW, Spijkers P, Guo H, Song X, Lenting PJ, Van Nostrand WE, Zlokovic BV. LRP/amyloid β-peptide interaction mediates differential brain efflux of Aβ isoforms. Neuron 2004;43:333–344. [PubMed: 15294142]

DeMattos, RB.; Bales, KR.; Paul, SM.; Holtzman, DM. Potential role of endogenous and exogenous Aβ binding molecules in Aβ clearance and metabolism. In: Saido, T., editor. Aβ metabolism in Alzheimer's disease. Bioscience; Landis: 2003. p. 123-129.

DeMattos RB, Cirrito JR, Parsadanian M, May PC, O'Dell MA, Taylor JW, Harmony JA, Aronow BJ, Bales KR, Paul SM, Holtzman DM. ApoE and clusterin cooperatively suppress Aβ levels and

NIH-PA Author Manuscript NIH-PA Author Manuscript NIH-PA Author Manuscript

NIH-PA Author Manuscript

deposition: evidence that apoE regulates extracellular Aβ metabolism *in vivo*. Neuron 2004;41:193–202. [PubMed: 14741101]

DeMattos RB, O'Dell MA, Parsadanian M, Taylor JW, Harmony JA, Bales KR, Paul SM, Aronow BJ, Holtzman DM. Clusterin promotes amyloid plaque formation and is critical for neuritic toxicity in a mouse model of Alzheimer's disease. Proc Natl Acad Sci USA 2002;99:10843–10848. [PubMed: 12145324]

Fryer JD, DeMattos RB, McCormick LM, O'Dell MA, Spinner ML, Bales KR, Paul SM, Sullivan PM, Parsadanian M, Bu G, Holtzman DM. The low density lipoprotein receptor regulates the level of central nervous system human and murine apolipoprotein E but does not modify amyloid plaque pathology in PDAPP mice. J Biol Chem 2005;280:25754–25759. [PubMed: 15888448]

Gelfanova V, Higgs RE, Dean RA, Holtzman DM, Farlow MR, Siemers ER, Boodhoo A, Qian YW, He X, Jin Z, Fisher DL, Cox KL, Hale JE. Quantitative analysis of amyloid-beta peptides in cerebrospinal fluid using immunoprecipitation and MALDI-TOF mass spectrometry. Anal Biochem. 2006 (in press).

Ghersi-Egea JF, Gorevic PD, Ghiso J, Frangione B, Patlak CS, Fenstermacher JD. Fate of cerebrospinal fluid-borne amyloid β-peptide: rapid clearance into blood and appreciable accumulation by cerebral arteries. J Neurochem 1996;67:880–883. [PubMed: 8764620]

Ghilardi JR, Catton M, Stimson ER, Rogers S, Walker LC, Maggio JE, Mantyh PW. Intra-arterial infusion of [125I] Aβ 1-40 labels amyloid deposits in the aged primate brain *in vivo*. Neuroreport 1996;7:2607–2611. [PubMed: 8981432]

Hardy J, Selkoe DJ. The amyloid hypothesis of Alzheimer's disease: progress and problems on the road to therapeutics. Science 2002;297:353–356. [PubMed: 12130773]

Holtzman, DM.; Zlokovic, BV. Role of Aβ transport and clearance in the pathogenesis and treatment of Alzheimer's disease. In: Sisodia, S.; Tanzi, R., editors. Alzheimer's Disease: Advances in Genetics, Molecular and Cellular Biology. Springer; 2006. Chapter 11 (in press)

Iwata N, Tsubuki S, Takaki Y, Watanabe K, Sekiguchi M, Hosoki E, Kawashima-Morishima M, Lee HJ, Hama E, Sekine-Aizawa Y, Saido TC. Identification of the major Abeta1-42-degrading catabolic pathway in brain parenchyma: suppression leads to biochemical and pathological deposition. Nat Med 2000;6:143–150. [PubMed: 10655101]

Iwata N, Tsubuki S, Takaki Y, Shirotani K, Lu B, Gerard NP, Gerard C, Hama E, Lee HJ, Saido TC. Metabolic regulation of brain Aβ by neprilysin. Science 2001;292:1550–1552. [PubMed: 11375493]

Koistinaho M, Lin S, Wu X, Esterman M, Koger D, Hanson J, Higgs R, Liu F, Malkani S, Bales KR, Paul SM. Apolipoprotein E promotes astrocyte colocalization and degradation of deposited amyloid-β peptides. Nat Med 2004;10:719–726. [PubMed: 15195085]

LaRue B, Hogg E, Sagare A, Jovanovic S, Maness L, Maurer C, Deane R, Zlokovic BV. Method for measurement of the blood-brain barrier permeability in the perfused mouse brain: application to amyloid-β peptide in wild type and Alzheimer's Tg2576 mice. J Neurosci Methods 2004;138:233–242. [PubMed: 15325132]

Mackic JB, Stins M, McComb JG, Calero M, Ghiso J, Kim KS, Yan SD, Stern D, Schmidt AM, Frangione B, Zlokovic BV. Human blood-brain barrier receptors for Alzheimer's amyloid- β 1-40: asymmetrical binding, endocytosis and transcytosis at the apical side of brain microvascular endothelial cell monolayer. J Clin Invest 1998a;102:734–743. [PubMed: 9710442]

Mackic JB, Weiss MH, Miao W, Kirkman E, Ghiso J, Calero M, Bading J, Frangione B, Zlokovic BV. Cerebrovascular accumulation and increased blood-brain barrier permeability to circulating Alzheimer's amyloid-β peptide in aged squirrel monkey with cerebral amyloid angiopathy. J Neurochem 1998b;70:210–215. [PubMed: 9422364]

Maness LM, Banks WA, Podlisny MB, Selkoe DJ, Kastin AJ. Passage of human amyloid-β protein 1-40 across the murine blood-brain barrier. Life Sci 1994;55:1643–1650. [PubMed: 7968239]

Martel CL, Mackic JB, Matsubara E, Governale S, Miguel C, Miao W, McComb JG, Frangione B, Ghiso J, Zlokovic BV. Isoform-specific effects of apolipoproteins E2, E3, E4 on cerebral capillary sequestration and blood-brain barrier transport of circulating Alzheimer's amyloid β. J Neurochem 1997;69:1995–2004. [PubMed: 9349544]

Morikawa M, Fryer JD, Sullivan PM, Christopher EA, Wahrle SE, DeMattos RB, O'Dell MA, Fagan AM, Lashuel HA, Walz T, Asai K, Holtzman DM. Production and characterization of astrocyte-

NIH-PA Author Manuscript

NIH-PA Author Manuscript

NIH-PA Author Manuscript

derived human apolipoprotein E isoforms from immortalized astrocytes and their interactions with amyloid-β. Neurobiol Dis 2005;19:66–76. [PubMed: 15837562]

Poduslo JF, Curran GL, Haggard JJ, Biere AL, Selkoe DJ. Permeability and residual plasma volume of human, Dutch variant, and rat amyloid β-protein 1-40 at the blood-brain barrier. Neurobiol Dis 1997;4:27–34. [PubMed: 9258909]

Schmidt SD, Nixon RA, Mathews PM. ELISA method for measurement of amylod-β levels. Methods Mol Biol 2005;299:279–297. [PubMed: 15980612]

Selkoe DJ. Clearing the brain's amyloid cobwebs. Neuron 2001;32:177–180. [PubMed: 11683988]

Shibata M, Yamada S, Kumar SR, Calero M, Bading J, Frangione B, Holtzman DM, Miller CA, Strickland DK, Ghiso J, Zlokovic BV. Clearance of Alzheimer's amyloid-β 1-40 peptide from brain by LDL receptor-related protein-1 at the blood-brain barrier. J Clin Invest 2000;106:1489–1499. [PubMed: 11120756]

Tanzi RE, Moir RD, Wagner SL. Clearance of Alzheimer's Aβ peptide: the many roads to perdition. Neuron 2004;43:605–608. [PubMed: 15339642]

Wyss-Coray T, Loike JD, Brionne TC, Lu E, Anankov R, Yan F, Silverstein SC, Husemann J. Adult mouse astrocytes degrade amyloid-β in vitro and in situ. Nat Med 2003;9:453–457. [PubMed: 12612547]

Zlokovic BV. Clearing amyloid through the blood-brain barrier. J Neurochem 2004;89:807–811. [PubMed: 15140180]

Zlokovic BV. Neurovascular mechanisms of Alzheimer's neurodegeneration. Trends Neurosci 2005;28:202–208. [PubMed: 15808355]

Zlokovic BV, Deane R, Sallstrom J, Chow N, Miano J. Neurovascular pathways and Alzheimer amyloid β-peptide. Brain Pathol 2005;15:78–83. [PubMed: 15779240]

Zlokovic BV, Ghiso J, Mackic JB, McComb JG, Weiss MH, Frangione B. Blood-brain transport of circulating Alzheimer's amyloid ß. Biochem Biophys Res Comm 1993;197(3):1034–1040. [PubMed: 8280117]

Zlokovic BV, Martel CL, Matsubara E, McComb JG, Zheng G, McCluskey RT, Frangione B, Ghiso J. Glycoprotein 330/megalin: probable role in receptor-mediated transport of apolipoprotein J alone and in a complex with Alzheimer's disease amyloid-β at the blood-brain and blood-cerebrospinal fluid barriers. Proc Natl Acad Sci USA 1996;93:4229–4234. [PubMed: 8633046]

NIH-PA Author Manuscript

NIH-PA Author Manuscript

NIH-PA Author Manuscript

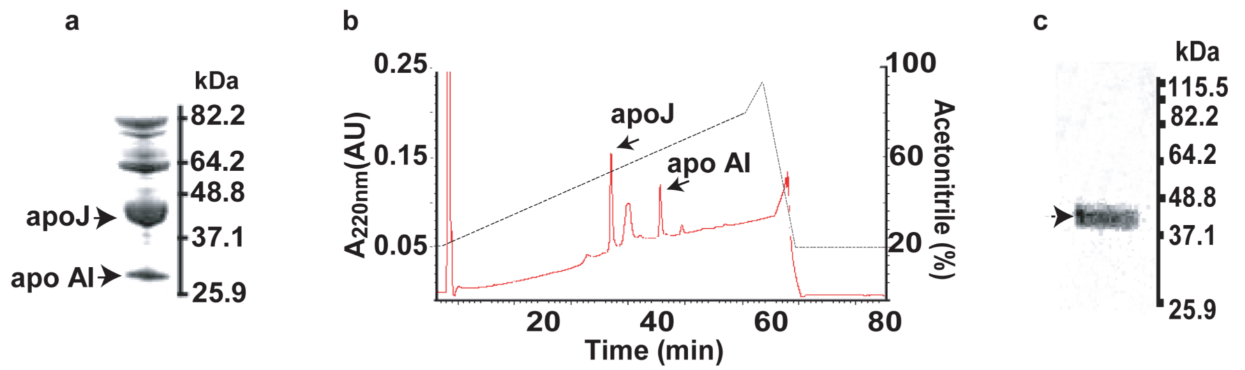

Fig. 1.

a, SDS-PAGE analysis of crude extract of human plasma apoJ. ***b***, HPLC purification of the crude apoJ extract. ***c***, SDS-PAGE analysis of the apoJ peak in *b* (reduced conditions). ApoAI, apolipoprotein A one.

NIH-PA Author Manuscript

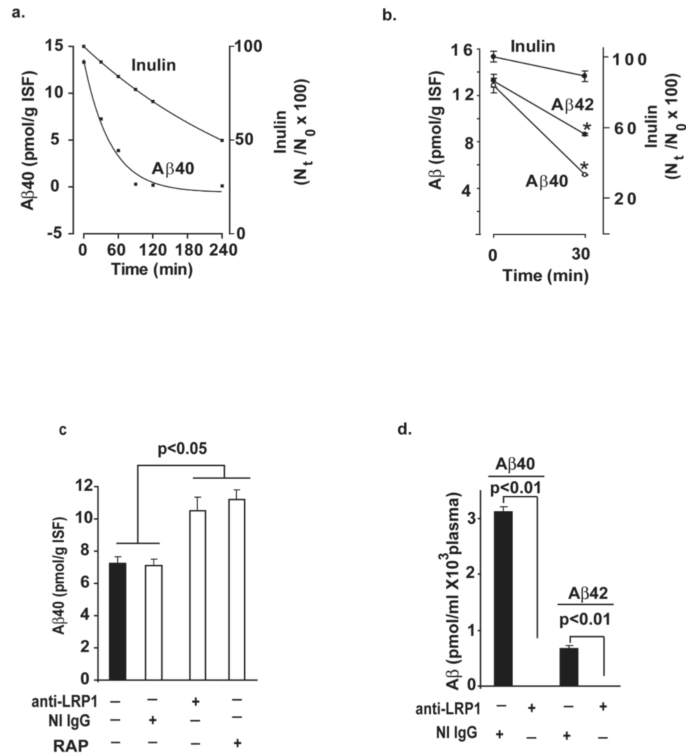

Fig. 2.

a, Time-disappearance curves of unlabeled human Aβ40 (0.0866 ng) and ^{14}C-inulin from brain ISF after their simultaneous administration into the caudate nucleus in mice. Each pair of time points represents data from individual mice for Aβ and inulin. ***b,*** Clearance of unlabeled human synthetic Aβ40 and Aβ42 from brain ISF within 30 min of administration into the caudate nucleus. Aβ40 and Aβ42 were infused simultaneously with ^{14}C-inulin. ***c,*** Levels of Aβ40 in brain after 30 min of its simultaneous administration with inulin (not shown) in the presence and absence of anti-LRP1 (N-20, 60 μg/mL), non-immune IgG (60 μg/mL) and RAP (5 μM). ***d,*** Intact human unlabeled Aβ40 and Aβ42 in plasma 30 min after local CNS administration of peptides simultaneously with ^{14}C-inulin in the presence and absence of centrally administered anti-LRP1 (N-20, 60 μg/mL). Inulin levels were barely detectable (not shown). Aβ levels were determined focally in brain and plasma by using human specific ELISAs, as described in Methods. In *b-d*, values are mean ± s.e.m. from 3 to 5 independent experiments.

NIH-PA Author Manuscript

NIH-PA Author Manuscript

NIH-PA Author Manuscript

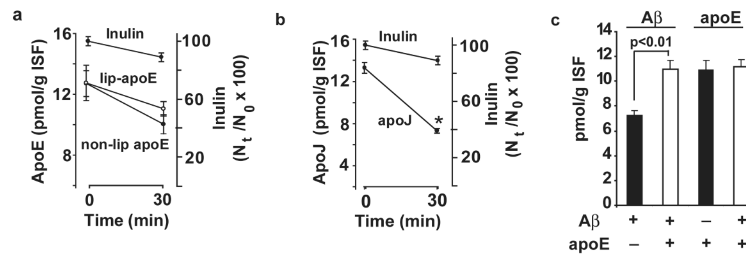

Fig. 3.

a, Clearance of unlabeled human apoE (isoform 3; 0.70 ng), non-lipidated and lipidated, from brain ISF within 30 min of administration into the caudate nucleus. ApoE was infused simultaneously with ^{14}C-inulin. ***b,*** Clearance of native human apoJ (1.6 ng) from brain ISF within 30 min of its simultaneous administration into the caudate nucleus with ^{14}C-inulin. ***c,*** Clearance of unlabeled Aβ40 and apoE (isoform 3) administered into brain ISF simultaneously with ^{14}C-inulin either alone (closed bars) or in the form of Aβ- apoE complex (open bars). Inulin values not shown. ApoE, apoJ and Aβ levels were determined focally in brain and plasma by using human specific ELISAs, as described in Methods. Values are mean ± s.e.m. from 3 to 5 independent experiments.

NIH-PA Author Manuscript
NIH-PA Author Manuscript
NIH-PA Author Manuscript

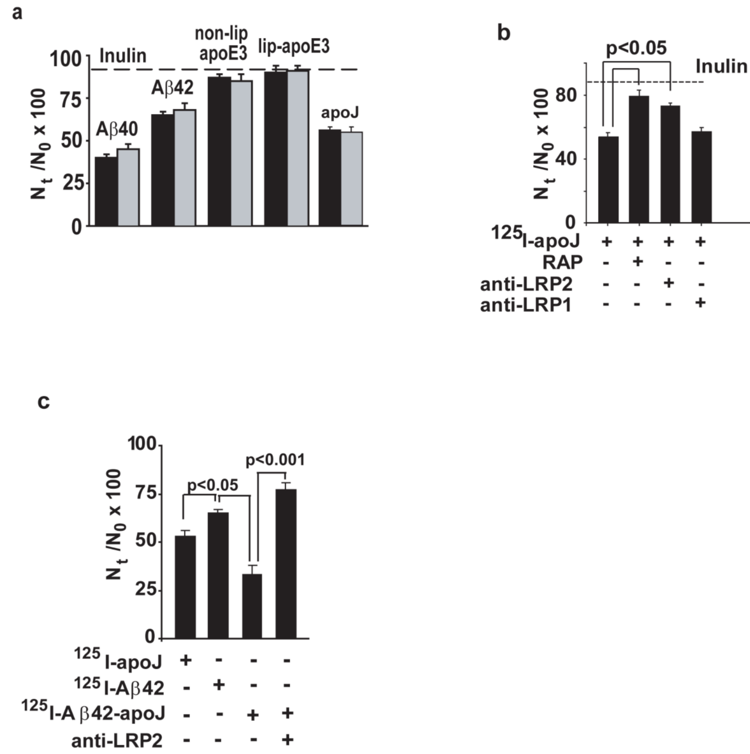

Fig. 4.

a, Brain clearance of unlabeled (*solid bars*) and ^{125}I-labeled (*open bars*) Aβ and apolipoproteins from brain ISF. The same amounts of unlabeled and the respective ^{125}I-labeled Aβ40, Aβ42, apoE non-lipidated and lipidated isoform 3 and apoJ were infused with ^{14}C-inulin into brain ISF in the caudate nucleus. The levels of unlabeled Aβ and apoE were determined by human specific ELISAs (*solid bars*) and of ^{125}I-labeled Aβ and apoE by gamma counting (*open bars*). The percentage recovery was calculated as $N_t/N_0 \times 100$ (eq. 1, Methods). Mean ± s.e.m., n = 3-8. ***b,*** Clearance of ^{125}I-apoJ (1.6 ng/0.5 μL; TCA-precipitable radioactivity) in the absence and presence of RAP (5 μM), anti-LRP-2 (Rb 6286, 60 μg/ml, from Dr. S. Argraves) and anti-LRP-1 (N20, 60 μg/ml) simultaneously infused with ^{14}C-inulin. ***c,*** Effects of apoJ on ^{125}I-Aβ42 clearance from brain ISF and effect of anti-LRP2 (Rb 6286, 60 μg/ml). For *b-c*, values are mean ± s.e.m., n = 3-5.

NIH-PA Author Manuscript

NIH-PA Author Manuscript

NIH-PA Author Manuscript

Table 1

Clearance rates of unlabeled Aβ, apoE and apoJ across the BBB and via the ISF flow.

Clearance rates (pmol/min/g ISF)		
Non-labeled molecules	**Transport via BBB**	**Transport via ISF**
A β 40	0.211 ± 0.022	0.034 ± 0.004
A β 42	0.111 ± 0.011	0.031 ± 0.002
non-lip-apoE3	0.041 ± 0.003	0.030 ± 0.003
lip-apoE3	non-detectable	0.035 ± 0.005
apoJ	0.163 ± 0.013	0.037 ± 0.003
A β 40-apoE	0.037 ± 0.003 *	0.034 ± 0.003

Values were calculated with eqs. 2,4, and 5; Mean ± s.e.m. from 6-8 mice per test molecule.

*p<0.01, Aβ40-apoE compared to Aβ40. Non-lip-apoE3, lipid-poor apoE3; lip-apoE3, lipidated apoE3.

NIH-PA Author Manuscript
NIH-PA Author Manuscript
NIH-PA Author Manuscript

Table 2

Clearance rates of ^{125}I-labeled Aβ, apoE and apoJ across the BBB and via the ISF flow.

Clearance rates (pmol/min/g ISF)		
^{125}I-labeled molecules	**Transport via BBB**	**Transport via ISF**
A β 40	0.214 ± 0.020	0.030 ± 0.001
A β 42	0.101 ± 0.014	0.029 ± 0.001
non-lip-apoE3	0.036 ± 0.003	0.028 ± 0.002
lip-apoE3	non-detectable	0.035 ± 0.004
apoJ	0.155 ± 0.009	0.033 ± 0.004
Aβ42-apoJ	0.185 ± 0.009 *	0.031 ± 0.003

Values were calculated with eqs. 2,4, and 5; Mean ± s.e.m. from 6-8 mice per test molecule.

* $p<0.01$, Aβ42-apoJ compared to Aβ42. Non-lip-apoE3, lipid-poor apoE3; lip-apoE3, lipidated apoE3.